50 KRPM, 1,100°F MAGNETIC BEARINGS FOR JET TURBINE ENGINES

Mouhoub Mekhiche, Stephen Nichols, John Oleksy, John Young, Jerome Kiley, Douglas Havenhill
SatCon Technology Corp., 161 First St., Cambridge, MA 02142, USA, mekhiche@satc.com;

ABSTRACT
The need for an increased jet turbine engines' propulsion capability requires: (1) lightweight, (2) high-efficiency, (3) high-speed and (4) high-temperature components. These requirements put the conventional components such as the mechanical bearings under excessive constraints and make them obsolete. In this context, SatCon Technology Corporation has developed a high-speed, high-temperature (50 krpm, 600°C) magnetic bearing system that has the potential of meeting these requirements. This magnetic bearing system, comprised of two radial and one double acting thrust bearings, was successfully tested to 50,000 rpm. This paper describes the development of this system from its design through its fabrication and testing. Details on the system and component requirements are presented, along with a step-by-step design and trade-off analysis. Test data and their discussion are provided, as well.

INTRODUCTION

Magnetic bearings have been identified as one of the key electro-mechanical system components required for achieving the performance increase to double the propulsion capability of turbine engines. As higher working temperatures and speeds, lighter weight and more efficient components are required, classical (mechanical) bearings become unsatisfactory and, thus, more creative approaches are sought. Magnetic bearings are key to achieving the performance increase set by the jet turbine engine industry since their use leads to the following:

- Efficiency will improve due to the elimination of rolling elements, drag and oil pumping
- Achievable shaft speed will increase with the elimination of the surface speed limitations of rolling-element bearings
- Weight is reduced by the elimination of internal and external piping for lubricants with an associated simplification of mechanical and aerodynamic designs
- Maintenance costs will be reduced since magnetic bearings do not wear and therefore require less frequent maintenance and part replacement.
- Reduced friction allows reduction of size and costs of starter drive.
- Reliability will improve
- Magnetic bearings can be made to operate at much higher temperatures than anti-friction or other mechanical bearings.

When designed to withstand extreme temperatures, magnetic bearings allow for a considerable reduction of engine size and increased reliability.

There has been some recent success at demonstrating various aspects of magnetic bearings for gas turbine engines, particularly those related to high-speed operation. Several ongoing efforts are addressing the component and system aspects of the technology required to develop a magnetic bearing system that incorporates all of the necessary efficiency and robustness for a man rated aircraft engine. In particular, two key components have yet to be achieved. These components are flight weight radial and axial magnetic bearing actuators that can survive under high temperature and extreme loads while maintaining speed and efficiency.

In this context, a magnetic bearing system that meets the requirements for the working conditions of a jet turbine engine from the standpoint of speed (50,000 rpm) and temperature (600°C) is being developed. This research is under a contract with the United States Army. In the following, details of the design are presented along with the hardware fabrication and testing.

DESIGN PROCEDURE AND HARDWARE

The classical goal of magnetic bearing technology has been, up until now, the demonstration of a weight optimized magnetic actuator at realistic engine temperatures. In order to achieve that desired goal, several research programs were defined to develop high-temperature magnetic bearings. The wide majority of these programs seem to have taken similar, if not identical, approaches to magnetic actuator design and fabrication. These high-temperature actuators featured eight or twelve pole, hetero-polar geometry using welded Cobalt-steel stacks and ceramically encased copper conductors.

Our approach towards solving the high-speed, high-temperature, light weight and high-efficiency magnetic bearing design and fabrication problem is different in the following way: it considers and accounts for multiple aspects of the design process and requirements in a simultaneous fashion. In effect, when faced with requirements for high load capacity in a tightly constrained volume (i.e., high-force density) at high temperature, the design paradigm described above does not work very well. To describe the difficulty, it is instructive to consider three key aspects of developing light, small and high-force density electromagnetic devices. These apply equally to high power density rotating electric machinery and to high force-density magnetic actuators:

a. Select the "best" magnetic materials: Soft-iron cores should employ material with high saturation flux density (subject on limitations on core losses) while conductor materials must have low resistivity to allow high current density with tolerable ohmic dissipation.

b. Control environmental conditions: Mechanisms must be employed to transfer waste heat out of core stacks and coil bundles to maintain component temperatures within prescribed operating limits. Mechanical stresses must be managed by structural design to be below safe operating levels for all components.

c. Optimize the magnetic circuit: The sizes of the various magnetic components must be adjusted so as to make best use of the capacity of all materials. For instance, under the maximum mechanical load, all core sections should be at or near flux saturation while the coils should be at their maximum current density.

Through the use of the design procedure described above, a magnetic bearing system (two radial bearings and one double acting thrust bearing) which meets the loading requirements at the prescribed temperatures, was designed. These actuators fit within the available bearing-compartment volume. During the course of the design effort, we re-assessed, reconsidered, and eventually rejected the "conventional" approach in favor of a more direct path to a high-temperature, high-speed working magnetic bearing system. For instance, classical approaches using heteropolar designs using permanent magnets were dismissed since high-temperatures prohibit the use of existing PM materials.

Magnetic Bearings Design

System Requirements and Specifications: The objective of this research work is to validate the innovations necessary for operation of magnetic bearings at high-speeds and high-temperatures by designing and fabricating a magnetic bearing system mounted in an appropriate test-rig to accurately simulate the operating conditions of a jet turbine engine. The requirements on this system are described in Table 1. The magnetic bearing system is comprised of two radial bearings corresponding to the hot and cold ends of the jet turbine engine that controls the radial positioning of the turbine shaft, and a thrust bearing that controls the axial play the engine.

A proprietary technology that allows for the fabrication of high-temperature tolerant coils was developed. The radial bearings, although identical from the design standpoint for symmetry purposes, were fabricated in different ways to meet temperature requirements.

TABLE 1. Magnetic Bearing System Requirements.

The magnetic bearing system shall be fault tolerant	
Coil inductance	10 mH
Coil resistance	2 Ohms
Cold end actuator max. load	1754 N
Cold end thrust max. load	5194 N
Cold end bearing temperature	300 ^{o}C
Hot end actuator max. load	1862 N
Hot end temperature	520 ^{o}C
Cold end actuator diameter	90 mm
Cold end axial length	73 mm
Hot end actuator diameter	81 mm
Hot end bearing axial length	81 mm
Weight	MINIMUM
Cooling	Air
Gravitational forces up to 9 times earth's gravity	

The design procedure was carried out in two stages: first an analytical design using linear analysis methods was implemented in a spreadsheet. The result is detailed information related to the size, shape, load, current density, impedance and efficiency of the actuators. In a second step, a detailed non-linear analysis using Finite Element based software (magnetic, mechanical, and thermal) was carried out to validate and/or apply the necessary modifications to the preliminary design in order to improve actuator performance.

The final design of the various actuators is summarized in the following sections.

Radial Bearings. The radial bearings, although identical in design for symmetry purposes and rotor-dynamics improvement, were fabricated in different ways to meet temperature requirements (Figs. 1 and 2). The parameters of Table 2 were obtained through the analytical design, while Fig. 3 is an example of a FEA analysis showing the flux density distribution of the actuator under maximum load. This analysis is critical as it allows for the choice of appropriate magnetic materials that would simultaneously withstand the working temperature while delivering the required flux density.

TABLE 2. Final design of radial bearings.

Parameter	Radial bearing position
Operating gap	0.5 mm”
Maximum required MMF	1630 A-turns
Saturation flux	2.0 T
Bias flux density	1.1 T
Back iron width	0.281”
Peak coil current density	850 A/cm^2
Rotational losses at max load, 50 krmp	512 W

Thrust Bearing. The same procedure was applied in the design of a double acting thrust bearing to compensate for axial loads as high as 5243 N. The main parameters of this axial bearing are presented in Table 3.

TABLE 3: Double acting thrust bearing parameters

Operating gap	0.5 mm
Saturation flux density	2 T
Magneto-motive force	1620 A-turns
Peak coil current density	320 A/cm^2
Thrust disk outer diameter	152.4 mm
Thrust disk axial length	12.7 mm

Test Rig Design and Topology

The two radial bearings and the double acting thrust bearing were mounted on a test-rig (Fig. 5) and support a 14kg-rotating shaft. This test-rig was designed to allow enough flexibility in performing various tests such as two and five degrees of freedom testing at high-temperature and high-speed. An air-turbine is used to bring the system to operating speeds. High-temperature sensors specifically developed for this application were used.

A removable oven designed to simulate the high temperature of the hot-end of the jet turbine is used to apply various levels of temperatures on the hot-end radial bearing (right-side of the picture), while the double acting thrust bearing is mounted at the end of the cold-end if the test-rig (left side of the picture).

Controls Design

The magnetic bearing system has four unidirectional magnetic force actuators at each radial bearing location and two unidirectional magnetic force actuators in the axial direction.

The unidirectional actuators are operated differentially to produce bi-directional forces. The force output of the actuators is a nonlinear function of current and gap approximated as

$$F = K_f \quad \frac{i_1^2}{\left(1 \quad \frac{dg}{g_0}\right)^2} \quad \frac{i_2^2}{\left(1+\frac{dg}{g_0}\right)^2} \qquad (1)$$

where,

K_f is the force constant of the actuator at gap center (lbs/A^2)

i_i is the current in the positive direction actuator

i_2 is the current in the negative direction actuator

g is the rotor motion measured from gap center

g_0 is the distance from the pole face to the rotor at gap center

A common way to control this type of magnetic force actuator is to introduce a linearization bias using either a permanent magnet or by flowing a bias current through each coil. In our application, permanent magnets will not withstand the extreme temperatures. Bias currents cause steady state power dissipation that exacerbates an already severe thermal environment. Additionally, this control scheme introduces a negative spring constant which may require a high bandwidth control to overcome. Thus, we elected to use a nonlinear control. Using Eq. (1), an algorithm for computing the current in each actuator coil was derived and is shown below.

$$i_1 = \sqrt{\frac{(F_c + F_o)}{K_f g_0^2}}(g_0 \quad dg)$$

$$i_2 = \sqrt{\frac{F_o}{K_f g_0^2}}(g_0 + dg)$$

if (Fc<0)

$$i_2 = \sqrt{\frac{(F_o \quad F_c)}{K_f g_0^2}}(g_0 + dg)$$

$$i_1 = \sqrt{\frac{F_o}{K_f g_0^2}}(g_0 \quad dg)$$

where,

Fc is the force command

F_0 is a small bias force (20 N)

The algorithm works by first determining the sign of the force command and routing the current to the appropriate actuator. A small bias force is added to each actuator so the incremental gain of the square root function remains finite. The rest of the current calculation is straight forward. A high bandwidth current amplifier is used to apply the desired currents to the actuator coils.

Global Control vs. Local Control
The magnetic bearing system has six rigid body degrees of freedom, three translations and three rotations. From basic control theory we know that six bidirectional forces or torques arranged in such a way that they are not colinear and do not intersect in a point are required to fully control a rigid body. Fig. 1 is a sketch of the magnetic bearing system's rotor showing the forces acting on the rotor. The hot end radial actuators and cold end radial actuators each produce two bidirectional forces in the x-y plane and the axial actuators produces bidirectional forces in the z direction. This arrangement allows control of five degrees of freedom. An air turbine controls the remaining degree of freedom (rotation about the z axis). Therefore, 5 bidirectional forces and one torque and control the rigid body.
Similarly, measuring the motion of a rigid body requires the same number of bidirectional measurements as degrees-of-freedom. The magnetic bearing system has two bidirectional position sensors in the x-y plane outboard of the hot end radial actuators, two sensors in the x-y plane inboard of the cold end sensors, and one position sensor along the z-axis providing a five degree-of-freedom measurement of the motion of the rotor (Figure 7).
There are two basic control schemes commonly used in magnetic suspension, local control and global control. In local control a servo loop controls the rotor motion by sensing the actuator gap motion and applying current to the force actuator to cancel the gap motion. In global control, the motion of the center-of-mass of the rigid body is calculated from the position sensors and forces and torques required to zero-out the translational and rotational motions of the center-of-mass are calculated. Then the actuator forces required to produce the desired forces and torques are calculated. Local control has the advantage of simplicity; however, it has very little flexibility in how the rotor is controlled. Global control allows the control system's designer the flexibility to control each degree-of-freedom independently. Therefore, we elected to use global control.
A top level block diagram of the control law is shown in Fig. 8. The gap sensors measure the motion of the rotor. The B^1 matrix transforms the gap measurements into center-of-mass translations and rotations. Proportional plus integral plus lead lag control laws calculate the forces at and the torques about the center-of-mass required for rotor suspension. The A^{-1} matrix calculates the actuator forces required to produce the desired rigid body forces and torques. The current calculation block uses the force commands and the gap measurements to calculate the current required in each actuator to produce the desired force. The output of the current calculation is fed to current amplifiers that apply current to the actuators to produce force. The magnetic bearings system's plant is simply modeled as a six degree-of-freedom rigid body.

TEST DESCRIPTION: RESULTS AND DESCRIPTION

Prior to testing the magnetic bearing system at required temperature and speeds, static tests designed to characterize the various actuator force capabilities were performed. The results of these tests (see Actuator Force Characterization section) are recalled and discussed as well as the high speed ambient temperature testing (see the following). As this program is active, the high temperature tests are currently being done.

Actuator Force Characterization
Force Mapping Results: The purpose of this test is to evaluate the static load capability of the bearings in both the radial direction (x-y plan) and axial direction (z). In order to carry out this test, the rig was mounted on the table of a machine shop milling machine. A six-degree of freedom force/torque sensor was mounted to the head of the mill. Great care was taken to align the rotor so that we started in the center of the gap.

Test Procedure
Radial Actuators: Using a power supply and a current probe, current is applied to the hot end x or y axis coils. The measured force at each current level is recorded. When increasing the current level, the position sensors are monitored to insure that the rotor remains in the center of the gap. (Structural flexibility will allow gap motion with increasing force levels.)

Axial Actuator: Using a dial indicator, the rotor is set to the center of the gap in the axial direction. Various currents are applied in the outboard and inboard coils and the force applied by the actuators was measured. The currents and force at several current levels are recorded.
As shown in Fig. 9, the forces produced by the actuators obey the square law as a function of current. The maximum measured force is 980 N which corresponds to an actuator current of 7.2 A. The maximum design force is 1862 N (corresponding to 11.6 A). Extrapolating from the test results by using the square law, a maximum force of 1903 N corresponding to the design requirements of the magnetic bearing system will be achieved with the remaining 4.4 A. One of the interesting results that this test revealed is that two coils of the double acting thrust bearing provide different forces for the same current. One plausible explanation is the interaction between the two-coil wound on the same magnetic core resulting in a transformer effect.

Spin-Up Test
Once the various actuators were fully characterized through the previously described tests, a high-speed ambient temperature test was performed. The target speed was 50000 rpm with rotor fully suspended (5 degrees of freedom). This test was successfully

completed and the following is a presentation of the various data collected while at maximum speed.
As can be seen in Fig. 10, all the actuators corresponding to the two radial bearings and the double acting thrust bearing performed according to expectations. The currents, the speed and the rotor position are regular and correspond to sine-like shape corresponding to the rotational movement of the test-rig rotor. Fig. 11 shows the rotor orbits at both ends (hot and cold ends). As can be seen, although the rotor is located in the same spatial area (between the first and fourth quadrants), the hot end orbit is not as regular as its counterpart at the opposite end. This is attributed to the structure (due to the fact that the V-bloc that supports the rig is closer to the hot end than to the cold one) of the test-rig (see Fig. 6) that induces a rigid body mode that leads to such a non-regular orbit.

CONCLUSIONS

Throughout this paper, the authors presented the development of a high-speed, high-temperature magnetic bearing system from design through to its testing. A speed record was achieved for the size of bearings and supported shaft described in this work and a second series of tests involving high-temperatures to fully demonstrate this technology is currently being carried out.

ACKNOWLEDGEMENT

This work was performed under contract No. DAAH10-98-C-0025, between the US Army-Aviation & Missile Command and SatCon Technology Corporation.

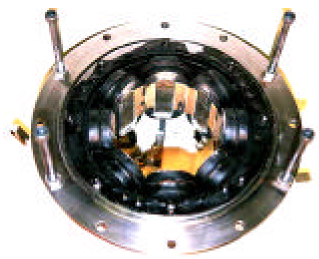

FIGURE 1: Hot end magnetic actuator

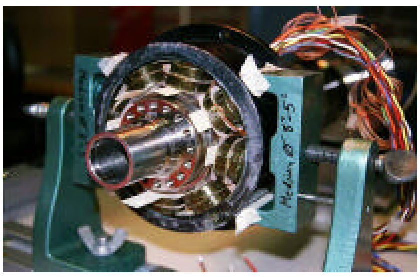

FIGURE 2: Cold end magnetic actuator

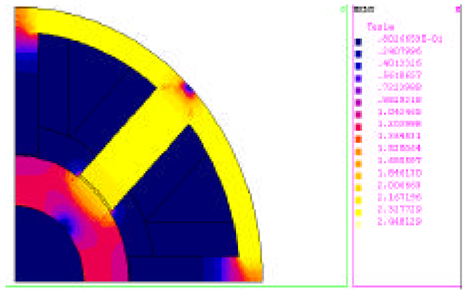

FIGURE 3: Magnetic flux density distribution under maximum load of the hot end radial bearing.

FIGURE 4: Final Test-Rig Topology

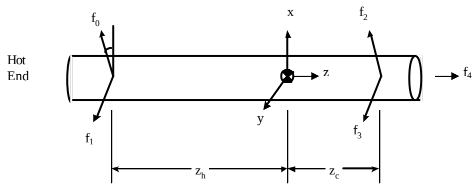

FIGURE 5: Magnetic Bearing System Force Actuator Geometry

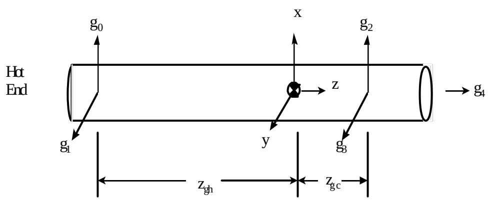

FIGURE 6: Magnetic Bearing System Position Sensor Geometry

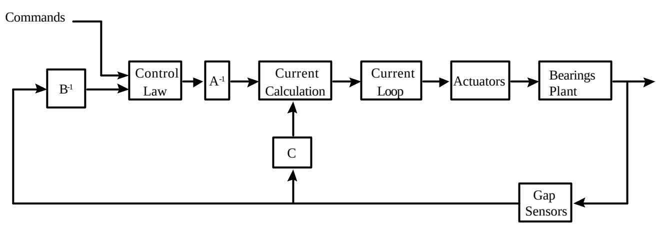

FIGURE 4: Magnetic Bearing Control System Block Diagram

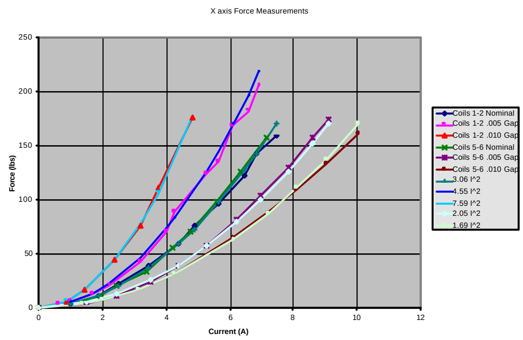

a.

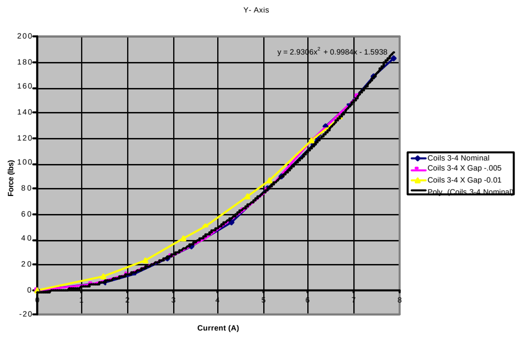

b.

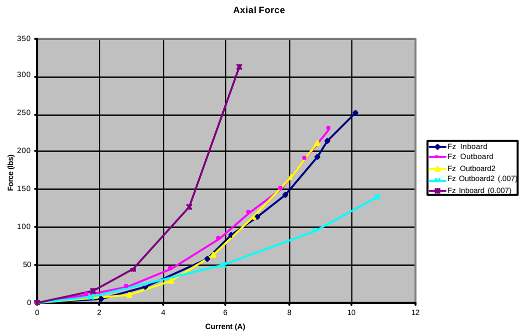

c.

FIGURE 9: Force mapping results:
(a): X-axis hot end radial bearing
(b):Y-axis: cold end radial bearing
© Z-axis: thrust (axial) bearing

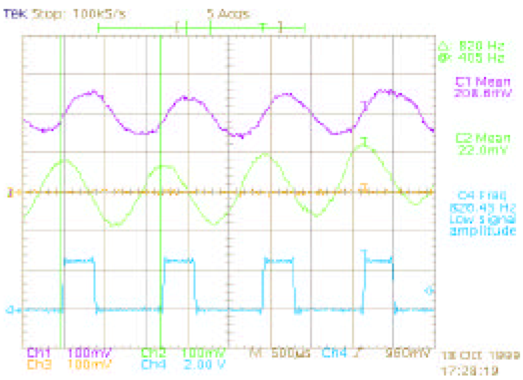

Cold end X-axis (ch1), Cold y (ch2) @ 50 krpm

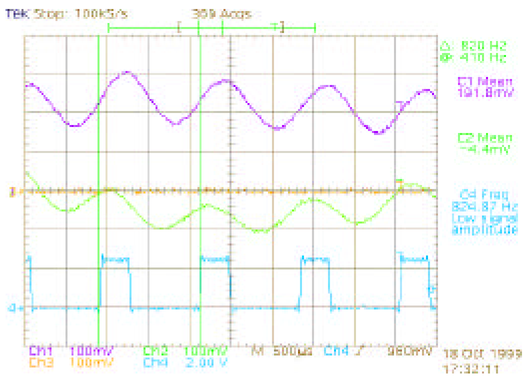

Hot x (ch1), Hot y (ch2) @ 50 krpm

FIGURE 10. Speed, current and position plots of the rotor and various actuators, respectively at 50,000 rpm

(Sensors scaled at 138 mV/mil) (Amplieiers scaled at 6V/20 Amps)

Thrust bearing (ch1) Amp9, (ch2) Amp 10, (ch3) @ 50 kpm

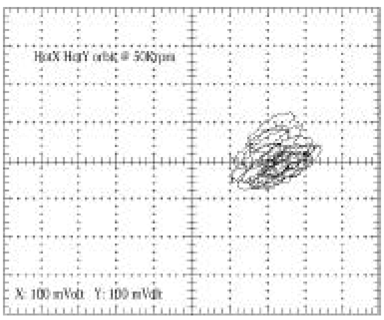

(Hot-end)

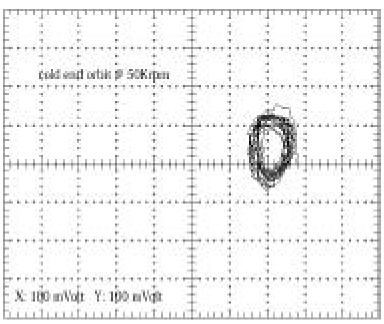

(Cold-end)

FIGURE 11: Orbit plots of the rotor while at 50000 rpm.